A Power Flow Method for Power Distribution Systems Based on a Sinusoidal Transformation to a Convex Quadratic Form

Jaber Valinejad, Student Member, IEEE, Lamine Mili, Life Fellow, IEEE, Yijun Xu, Member, IEEE

Abstract—The non-linearity and non-convexity of the AC power flow equations may induce convergence problems to the Newton-Raphson (NR) algorithm. Indeed, as shown by Thorp and Naqavi, the NR algorithm may exhibit a fractal behavior. Furthermore, under heavy loading conditions or if some of the line reactances are relatively large compared to the others, the Jacobian matrix becomes ill-conditioned, which may cause the divergence of this algorithm. To address the aforementioned problems for radial power distribution systems, we propose in this paper to apply a sinusoidal transform to map the AC power flow equations into a convex quadratic form, which includes nodebased and Pythagorean equations. The good performance of the proposed approach is demonstrated via simulations carried out on several power distribution systems.

Index Terms—Power flow; Sinusoidal transform; Fractal behavior; Quadratic form; Distribution systems.

Nomenclature

Indices

n/m	Bus n/m				
	Parameters				
p_n/q_n	The real/reactive power consumed at bus n				
R/X	The resistance/ reactance of transmission lines				
g_{nm}/g_l	The conductance of the transmission line be-				
	tween buses n and m/ of line l				
b_{nm}/b_l	The Suseptance of the transmission line be-				
	tween buses n and m/ of line l				
Variables					
P_n/Q_n	The real/reactive power produced at bus n				
V_n	The voltage magnitude of bus n				
θ_n	The voltage angle of bus n				
P_{nm}/P_l	The real power transferred between nodes n				
	and m/ through line l				
Q_{nm}/Q_l	The reactive power transferred between nodes				
	n and m/ through line 1				

I. Introduction
One of the main tools for power system operation and planning is the power flow algorithm. It is used in the study of resilience, reliability, and efficiency of power systems [1]. The AC power flow analysis consists of solving a series of nonlinear equations in order to determine the voltage magnitudes and angles at all buses, and then to calculate the active and reactive power flows and power injections in the system. It is conducted in both power transmission and distribution systems. In this paper, we will focus on power distribution

The work presented in this paper was funded by the National Science Foundation (NSF) under Grant No. 1917308.

J. Valinejad, L. Mili, and Y. Xu are with the Bradley Department of Electrical and Computer Engineering, Virginia Tech, Northern Virginia Center, Greater Washington D.C., VA 22043, USA (email:JaberValinejad,lmili,yijunxu@vt.edu).

XXX-1-7281-XXXX-8/20/\$31.00 © 2021 IEEE

systems because of their growing importance resulting from the increasing connection of renewable energy resources.

The AC power flow equations are non-linear and nonconvex [2]. To solve them, the literature suggests several deterministic and probabilistic methods. For instance, by applying the adaptive polynomial chaos-ANOVA method, Xu et [3] develops a probabilistic power flow method. The AC power flow methods based on the Newton-Raphson (NR) algorithm to solve the polar sinusoidal equations suffer from various problems, including sensitivity to initial conditions, ill-conditioning problems, and fractal behavior. For example, if the initial value is not selected properly, the algorithm may diverge. To address this problem, Tostado-Veliz et al. [4] use Bulirsch – Stoer approach, while Tang et al. [5] uses the trustregion techniques along with a least-square solution. To deal with the non-convexity of the power flow equations, various researchers propose a number of alternative techniques such as various linearization techniques, including DC power flow models, and diverse convexification methods. For example, Yang et al. [6], and Shchetinin et al. [7] use a linearization technique and Venzke et al. [8] provide a convex relaxation approach to solve the power flow equations. It turns out that the linear models may lead to incorrect values for the voltage magnitudes and the reactive power flows and power injections. Besides this problem, conventional methods based on the NR method may suffer from convergence problems due to illconditioning of the Jacobian matrix. This occurs when a power system either has large R / X ratios [9], or is heavy loaded, or has some lines with relatively large reactances as compared to the others. Another problem that the NR algorithm suffer from is a fractal behavior under certain conditions [10]. In power systems, this was demonstrated by Thorp and Naqavi [11]. To address all these problems, we propose in this paper to use a sinusoidal mapping to transform the power flow equations into a quadratic form for radial power distribution systems. The advantage of this sinusoidal mapping is that it makes the power flow equations quadratic, and hence convex, without using any approximations.

The rest of this paper is organized in the following way. Section II explores the polar-form AC power flow equations and explains the fractal property of the power flow equations solved by the NR algorithm. The new convex form is explored by means of a sinusoidal transform function in Section III. In section V, several case studies on a 22-bus and an 81-bus distribution system demonstrate the good performance of the proposed approach. Finally, the conclusions are provided in Section VI.

II. THE POWER FLOW NR ALGORITHM

We first present the polar form of the power flow equations and then discuss the NR algorithm's fractal behaviors.

A. Polar Form of the Power Flow Equations

By using the Ohm and Kirchhoff laws, real power, P_{nm} , and reactive power, Q_{nm} , are derived as follows:

$$P_{nm} = g_{nn}V_n^2 + g_{nm}V_nV_m\cos(\theta_n - \theta_m)$$

$$Q_{nm} = -b_{nn}V_n^2 + g_{nm}V_nV_m\sin(\theta_n - \theta_m);$$

$$Q_{nm} = -b_{nn}V_n^2 + g_{nm}V_nV_m\sin(\theta_n - \theta_m)$$
(1)

$$-b_{nm}V_nV_m\cos(\theta_n-\theta_m). (2)$$

Besides, the real and reactive power balance for each node is given by

$$P_{n} - p_{n} - g_{nn}V_{n}^{2} - \sum_{m=1(m\neq n)}^{N} g_{nm}V_{n}V_{m}cos(\theta_{n} - \theta_{m})$$

$$+b_{nm}V_{n}V_{m}sin(\theta_{n} - \theta_{m}) = 0; \quad \forall n \quad (3)$$

$$Q_{n} - q_{n} + b_{nn}V_{n}^{2} - \sum_{m=1(m\neq n)}^{N} g_{nm}V_{n}V_{m}Sin(\theta_{n} - \theta_{m})$$

$$-b_{nm}V_{n}V_{m}sin(\theta_{n} - \theta_{m}) = 0, \quad \forall n \quad (4)$$

We assume that we have n_P PV buses and n_Q PQ buses. The total number of buses is equal to N. At PV buses, only the voltage angle is an unknown state variable while at PQ buses, both the voltage magnitude and angle are unknown state variables. Hence, considering one of the PV buses as a slack bus, the total number of the unknown state variables is equal to $n_P + 2n_Q - 1$. Besides the polar form, the power flow equations can be expressed in the rectangular form. Both forms of power flow equations are non-linear and non-convex leading to difficulty in convergence and fractal behavior. In the next part, we analyze the fractal behavior of the NR algorithm when solving the AC power flow equations.

B. Fractal Property of the NR algorithm

A fractal object has similar patterns to its portion where the Hausdorff-Besicovitch fractal dimension noticeably surpasses the topological dimension [12]. Recall that the fractal dimension is the power of scale that is not necessarily an integer, while that of a geometric figure is always an integer number. Therefore, their scalability is different. The fractal dimension is obtained by $Log^N_\zeta=-D=\frac{LogN}{Log\zeta}$, where ζ is the scaling factor, D is the fractal dimension, and Nis the number of sticks. Fractals are not differentiable and cannot be measured in traditional ways. A fractal object's main characteristics are self-similarity, which means having a fine or detailed structure at arbitrarily small scales. Selfsimilarity, also known as an unfolding symmetry, can be found in one of the following categories: exact self-similarity, quasi self-similarity, qualitative self-similarity (in a time series), and multifractal scaling [13]. In addition to geometric patterns, fractals can also characterize stochastic processes. Fractal patterns with different degrees of self-similarity have been observed in various areas such as images, sounds, nature, technology, art, architecture, law, and numerical algorithms.

When the Newton algorithm is used to solve the power flow equations, it may experience a fractal behavior [11]. This may occur either under heavy loading conditions, or high values of one or several line reactances, or the choice of an inappropriate initial point. To show the fractal behavior of the power flow equations, we consider a simple three-machine system [11].

By selecting Bus 1 as the slack bus, we get the following power flow equations:

$$f_1(\theta_2, \theta_3) = 0.5 - 0.4\cos(\theta_2) - 1.9\sin(\theta_2) -0.2\cos(\theta_2 - \theta_3) - 2\sin(\theta_2 - \theta_3);$$
 (5)

$$f_2(\theta_2, \theta_3) = 3.9 - 1.6\cos(\theta_3) - 7.3\sin(\theta_3) + 0.2\cos(\theta_2 - \theta_3) + 2\sin(\theta_2 - \theta_3).$$
 (6)

The Julia set of power flow equations of 3 buses system, solved by the NR algorithm, is shown in Figure 1. The Hurst exponent, H, of these equations is equal to 0.83 for when $0 \le \delta 1, 2 \le 8\pi$. the fractal dimension, D, can be obtained by D = 2 - H. Hence, the fractal dimension is equal to 1.73. The fractal dimension shows the level of fractal behavior of the Julia set.

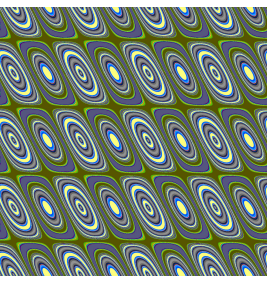


Fig. 1. The Julia set curves of the NR algorithm for a 3-bus power system when $0 \le \delta_{1,2} \le 8\pi$.

To address these challenges, we convert the non-convex power flow equations into a convex quadratic form by using a sinusoidal function transform as discussed next.

III. SINUSOIDAL FUNCTION TRANSFORM OF THE POWER FLOW EQUATIONS

This section discusses the foundation of the sinusoidal function transformation and how it converts the non-convex polar form of the power flow equations into a quadratic convex form.

A. Sinusoidal Function Transform

This transformation starts with the following two equations:

$$x_{a_l} = V_n \cos(\theta_n - \theta_m), \; \forall l$$
 (7)

$$x_{b_l} = V_n sin(\theta_n - \theta_m), \; \forall l$$
 (8)

where n is the line I that connects node n to node m. By using this definition, the non-convex equations 3 and 4 are converted into the convex form as follows

$$P_{n} - p_{n} - g_{nn}V_{n}^{2}$$

$$-\sum_{i=1,m\to i}^{l} g_{i}V_{m}x_{a_{i}} + b_{i}V_{m}x_{b_{i}} = 0; \quad \forall n$$

$$Q_{n} - q_{n} + b_{nn}V_{n}^{2}$$

$$-\sum_{i=1,m\to i}^{l} g_{i}V_{m}x_{b_{i}} - b_{nm}V_{m}x_{a_{i}} = 0; \quad \forall n$$
(10)

where $m \dashv l$ means m is the end node of line l. We will now check that the total number of the variables and equations in the new form are equal. To this end, we start by assuming that we have L lines. According to Eqs. (7) and (8), we have 2L state variables. In the new form, the voltage angles are no longer state variables, while the voltage magnitudes are state

variables. Hence, the total number of states variables is equal to $A=2L+N_Q$. In addition, according to Eqs. (9) and (10), we have $B = 2N_Q + N_P$ convex equations. The difference between the number of variables and equations is obtained by

$$A - B = 2L + N_Q - 2N_Q - N_P = 2L - N_Q - N_P.$$
 (11)

In radial distribution networks, L = N-1 since $N_P + N_Q =$ N-1. By leveraging these two relationships, the difference between the number of variables and equations is obtained by

$$A - B = 2L - (N_Q + N_P) = 2L - (N - 1) = L.$$
 (12)

This implies that L additional equations are needed when dealing with a radial distribution power system. These L equations are Pythagorean equations given by

$$x_{q_l}^2 + x_{h_l}^2 = V_n^2 . \forall l$$
 (13)

In addition, the real and reactive power flow equations in the new convex form are given by

$$P_{l} = g_{nn}V_{n}^{2} + g_{l}V_{m}x_{a_{l}} + b_{l}V_{m}x_{b_{l}}; \quad \forall l$$
 (14)

$$Q_{l} = -b_{nn}V_{n}^{2} + g_{l}V_{m}x_{b_{l}} - b_{l}V_{m}x_{a_{l}} = 0. \quad \forall l$$
 (15)

From our discussion, we infer that we have to first use Eqs. (7) and then (8) to convert the power flow equations to the new form. Then, we solve a set of convex equations as provided in Table 1.

TABLE I CONVEX POWER FLOW EQUATIONS USING A SINUSOIDAL TRANSFORMATION

Node-based equations:

$$P_n - p_n - g_{nn}V_n^2 - \sum_{i=1, m \to i}^l g_i V_m x_{a_i} + b_i V_m x_{b_i} = 0 \quad (16)$$

$$Q_n - q_n + b_{nn}V_n^2 - \sum_{i=1,m \to i}^l g_i V_m x_{b_i} - b_{nm}V_m x_{a_i} = 0$$
 (17)

Line-based equations (Pythagorean identity):

$$x_{a_l}^2 + x_{b_l}^2 - V_n^2 = 0 (18)$$

To solve these set of convex quadratic equations, we can use various approaches. In this paper, we apply the Trust-Region-Dogleg algorithm [14], [15].

B. Trust-Region-Dogleg Algorithm

For the Newton' method, the variable state x_{k+1} is obtained by

$$X_{k+1} = x_k + \Delta_k \tag{16}$$

 $0 = \Delta_k + J^{-1}F(x_k) \eqno(17)$ When the Jacobian matrix is singular, there is no value

for Δ_k . In addition, when the initial points are deviant, the Newton's method may diverge. The useful approach to deal with these challenges is the Trust-region algorithm [14]. According to this approach, we check if x_{k+1} is better than x_k or not via the function $G_k(x_k,$ which is defined as $G_k(x_k, \Delta_k) = \Delta_k + J^{-1}F(x_k),$

$$G_k(x_k, \Delta_k) = \Delta_k + J^{-1}F(x_k), \tag{18}$$

where
$$\Delta_k$$
 is given by
$$Min_{\Delta_k} = \frac{1}{2}G_k(x_k, \Delta_k)^T G_k(x_k, \Delta_k)$$
 (19)

To calculate Δ_k , the Powell-Dogleg procedure is used. Here, Δ_k is a combination of the Cauchy step, i.e, δ_c , and the Gauss-Newton step for $F(x_k)$, i.e, δ_{qn} . Δ_k is obtained by

$$\Delta_k = \delta_c + \alpha(\delta_{qn} - \delta_c), \tag{20}$$

where α gets a value between 0 and 1. The α is chosen such that Δ_k is less than a given threshold. The Cauchy step, i.e., δ_c and the Gauss-Newton step, i.e., δ_{qn} are obtained by

$$\delta_c = -\beta J^T F(x_k),\tag{21}$$

$$\delta_{qn} = -J^{-1}F(x_k),\tag{22}$$

where β minimizes Eq. (19). When the Jacobean matrix is singular, Δ_k is obtained via the Cauchy step. The detailed discussion is provide in [14], [15].

After solving the convex forms of the power flow equations using the trust-region-Dogleg algorithm, we calculate the voltage magnitudes, the real and reactive power lines, and the real and reactive power injections at the PV buses. Note that the voltage angle at the slack bus is set to zero, that is, θ_1 =0. First, we calculate the voltage angles of the buses that are connected to the slack bus and put them in the set Z. Then, we calculate the voltage angles of the buses that they are connected to the buses in set Z. We continue this process through forwarding substitution until all the bus voltage angles are calculated.

IV. REALISTIC DISTRIBUTION SYSTEMS A. 3-Phase Distribution Systems

The power flow equations for a 3-phase distribution system are given by

$$P_i^{inj,p} - V_i^p \sum_{q \in (a,b,c)} \sum_{j=1}^{N_{bus}} V_j^q Y_{ij}^{pq} cos(\theta_i^p - \theta_j^q - \psi_{ij}^{pq}) = 0, (23)$$

$$Q_i^{inj,p} - V_i^p \sum_{q \in (a,b,c)} \sum_{j=1}^{N_{bus}} V_j^q Y_{ij}^{pq} sin(\theta_i^p - \theta_j^q - \psi_{ij}^{pq}) = 0, (24)$$

where i and j are the bus numbers and a, b, and c are the bus phases. For this system, there are relationships between the cosine functions of angles, resulting in nine new convex equations according to various combinations of angles. By using the sinusoidal function transform discussed earlier, the final form of these equations are: $V_i^{a,b,c}x_1 = x_2x_3 + x_4x_5$, which have a convex quadratic form. Note that the proof is out of the scope of this paper.

B. Synchronous Generator-Based Distribution Generation

The real and reactive power generated by a droop-controlled synchronous generator-based DG's are expressed as

$$P_{G,i}^1 = \eta_i(w_{0,i} - w) \tag{25}$$

$$Q_{G,i}^1 = \mu_i (V_{0,i}^1 - |V_i^1|) \tag{26}$$

Considering the frequency as the variable in the power flow equations while using Eqs.(25) and (26) do not change their convex quadratic form. Note that the proof is out of the scope of this paper.

C. Distribution Systems With Various Load Models

1) Induction motors loads: As described in detail in [16], the real and reactive power consumed by the induction motors

$$P_{\text{trl}}^{\text{IM}} = \left(R_{1r}^s + \frac{R_{1r}^r}{S_r}\right) \cdot \frac{V_{\text{n}}^2}{\left(R_{1r}^s + \frac{R_{1r}^r}{S_r}\right)^2 + \left(X_{1r}^{\text{ys}} + X_{1r}^{\text{yr}}\right)^2} \tag{27}$$

$$Q_{\text{trl}}^{\text{IM}} = (X_{1r}^{\text{ys}} + X_{1r}^{\text{yr}}) \cdot \frac{V_{\text{n}}^{2}}{(R_{1r}^{s} + \frac{R_{1r}^{r}}{S_{1r}})^{2} + (X_{1r}^{\text{ys}} + X_{1r}^{\text{yr}})^{2}}$$

$$S_{1r} = \frac{(W_{1r}^{s} - W_{1r}^{r})}{W_{1r}^{s}}$$
(28)

2) Polynomial load model: As described in detail in [16], the real and reactive power consumed by a polynomial load

model are expressed as
$$P_{\rm n}^{\rm ZIP} = P_1 \left(\frac{V_{\rm n}}{V_{\rm n}^{\rm ref}}\right)^2 + P_2 \left(\frac{V_{\rm n}}{V_{\rm n}^{\rm ref}}\right) + P_3 \qquad (30)$$

$$Q_{\rm n}^{\rm ZIP} = Q_1 \left(\frac{V_{\rm n}}{V_{\rm ref}}\right)^2 + Q_2 \left(\frac{V_{\rm n}}{V_{\rm ref}}\right) + Q_3 \qquad (31)$$

$$Q_{\rm n}^{\rm ZIP} = Q_1 \left(\frac{V_{\rm ref}^{\rm ref}}{V^{\rm ref}}\right)^2 + Q_2 \left(\frac{V_{\rm ref}^{\rm ref}}{V^{\rm ref}}\right) + Q_3 \tag{31}$$

For these load models, the power flow equations maintain their convex quadratic form.

D. Meshed Distribution Systems



 θ_2 θ_4 e voltage angles are state Fig. 2. Meshed distribution systems where the

For meshed distribution systems, we can rewrite $\cos(\theta_3 - \theta_2)$ as $cos((\theta_3-\theta_1)+(\theta_1-\theta_2))$. Recall the following trigonometry identity: $cos(a+b) = cosa \ cosb - sina \ sinb$. By putting a = $\theta_3 - \theta_1$ and $b = \theta_1 - \theta_2$, we obtain a product of sine and cosine functions for each line. If we put $x_a = cosa$, and $x_b = sinb$, we get $x_{a3} = x_{a2}x_{a1} - x_{b1}x_{b2}$. Here, a3 means that a is related to Line 3. In general, we can write this equation as follows: $x_3 = x_2x_1 - x_4x_5$, which is convex quadratic.

V. CASE STUDIES

In this section, we use the proposed convex quadratic form to calculate the power flow equations of various case studies including, the 18-bus power distribution System [17], the 22-bus power distribution system [18], the 69-bus power distribution system [19], the 85-bus power distribution system [20], the 141-bus power distribution system [21], and the IEEE 906-bus European Test Feeder [22]. This section evaluates the performance of the convex quadratic form under heavy loads, large values of the line resistances and the reactances, and deviant initial points. To clarify the strength of the proposed model, we compare the convex quadratic form results to those of the conventional polar form. For both forms, we use the Trust-Region-Dogleg algorithm to solve the set of power flow non-linear equations.

1) Effect of Heavy Loads on the Power Flow Solutions: Table II provides the number of iterations, the residual, and the number of operations for various case studies for both the polar and the convex quadratic forms when the power system is under heavy loading conditions. Noe that the residual is the solution error upon convergence of the power flow algorithm. The simulations are performed for different cases as explained next. Firstly, we increase the load 4 times and then 32 times. When using the polar form, the residual significantly increases (e.g., 1.40×10^4 .), indicating that the power flow results are inaccurate. When the load in the 22-Bus power distribution system increases 32 times, the algorithm based on the polar form does not converge while when it is based on the convex quadratic form, it converges to an accurate solution. When the load in all the five tested distribution systems increases from

TABLE II POWER FLOW CALCULATION OUTPUTS FOR VARIOUS CASE STUDIES USING THE POLAR AND THE OUADRATIC FORM UNDER HEAVY LOADING CONDITIONS.

	Forms Case	Case study	Load growth	Iterations	Residual	Number of
	TOTHIS	Case study	Loud growth			operations
[18 - Bus Power	1	4	6.86e - 14	175
	-	Distribution	4	2862	65.518	100001
		System	32	2863	1.40 + 04	100002
		22 - bus Power	1	5	2.93e - 17	258
		Distribution	4	5	6.64e - 20	258
		System	32	-	-	-
	T	69 - bus Power	1	78	4.02e - 04	9735
	Polar form	Distribution	4	736	0.0737	100017
	7 7	System	32	744	31.735	100025
		85 - bus Power	1	5	2.61e - 12	1014
		Distribution	4	619	0.0209	100076
		System	32	594	1.476	100051
	θ_2	141 - bus Power	1	54	0.0024	13775
		Distribution	4	372	0.6562	100053
	_	System	32	473	1.07e + 02	100154
þ	cos (03- 02)	18 - Bus Power	1	4	5.03e - 22	260
IJ		Distribution	4	4	2.48e - 22	260
H		System	32	4	2.40e - 22	260
ı		22 - bus Power	1	5	3.46e - 14	384
		Distribution	4	5	3.67e - 14	384
	A	System	32	5	5.29e - 14	384
	Convex [©] θ Quadratic form	69 - bus Power	1	9	9.33e - 08	2050
de		Distribution	4	9	9.34e - 08	2050
		System	32	9	9.37e - 08	2050
		85 - bus Power	1	5	5.38e - 16	1518
		Distribution	4	5	5.51e - 16	1518
		System	32	5	7.65e - 16	1518
		141 - bus Power	1	16	4.16e - 11	6737
		Distribution	4	16	4.35e - 11	6737
		System	32	16	1.71e - 08	6737

1 to 4 to 32 times, the number of iterations of the algorithm based on the quadratic form remains constant. When the load in the 18-Bus power distribution system is increased 32 times, the residual of the polar form is 65.518 while that of the convex quadratic form is 2.48×10^{-22} . In other words, the residual has been improved by a factor of $3.785 \times 10^{+20}$, which is significant. As for the number of iterations and of operations, they have been decreased by a multiplicative factor of 715 and 384, respectively, in some scenarios. This demonstrates the excellent performance of the quadratic form under heavy loading conditions.

2) The Effect of the Increase of the Line Resistances and Reactances.: Table III provides the results of the power flow calculation based on the polar and the quadratic form when the line resistances or/and reactances are increased. We consider 5 scenarios for each case study of either form. For the 18bus and the 69-bus power distribution system, we increase the resistance or/and reactance of Line 3. Then, we increase the resistance or/and reactance of all the lines of the 141-bus power distribution system. In the polar form, residual increases significantly. For example, for the 18-bus power distribution system, when the reactance of Line 3 is increased 100 times, the residual of the algorithm based on the polar form amounts to 6.404 while that based on the quadratic form amounts to 9.41×10^{-15} . In other words, we improve the residual by a factor of $1.469 \times 10^{+15}$, which is significant. Furthermore, the algorithm based on the polar form does no converge scenarios 2-5 for the 69-bus power distribution system as described in Table III. According to the simulation results, the numbers of iterations and of operations have been improved by a factor 716, and 384 times in some scenarios. Obviously, when the line resistances or/and reactances are increased, the performance of the power flow calculations based on the

TABLE III
THE OUTPUTS OF THE POWER FLOW CALCULATIONS FOR VARIOUS
VALUES OF THE LINE RESISTANCES AND REACTANCES.

Forms	Case study	$R \times$	$X \times$	Iterations	REACTANCES Residual	Num. of Ope.
	10 D D	1	1	4	6.86e - 14	175
	18 – Bus Power Distribution System (Line 3)	1	100	2865	6.404	100004
		100	1	2865	2.835	100004
		100	100	2868	7.500	100007
		1e + 4	1e + 4	2867	12.799	100006
	69 – bus Power Distribution System (Line 3)	1	1	78	4.02e - 04	9735
		1	1e + 4	797	0.0658	100078
Polar form		1e + 4	1	-	-	-
P. G		1e + 4	1e+4	-	-	-
		1e + 6	1e+6	-	-	-
	141 - bus Power	1	1	54	0.0025	13775
		1	1e + 4	-	-	-
	Distribution System (All lines)	1e + 2	1	-	-	-
		1e + 2	1e + 4	-	-	-
		1e + 3	1e + 5	-	-	-
	18 – Bus Power	1	1	4	5.034e - 22	260
	Distribution System (Line 3)	1	100	4	9.41e - 15	260
		100	1	4	1.99e - 20	260
		100	100	4	2.31e - 14	260
	(Line 3)	1e + 4	1e + 4	8	2.16e - 10	468
	69 – bus Power Distribution System (Line 3)	1	1	9	9.33e - 08	2050
z iti c		1	1e + 4	11	1.65e - 08	2460
Convex Quadratic form		1e + 4	1	10	1.88e - 08	2255
ರಿ ಸ್ಥೆ ಆ		1e + 4	1e + 4	11	1.75e - 07	2460
		1e + 6	1e + 6	495	0.0037	100048
ļ	141 – bus Power Distribution System (All lines)	1	1	16	4.16e - 11	6737
		1	1e + 4	26	1.81e - 04	9267
		1e + 2	1	7	5.94e - 17	3368
		1e + 2	1e + 4	214	1.71e - 04	87995
		1e + 3	1e + 5	29	2.34e - 05	11370

TABLE IV
THE OUTPUTS OF THE POWER FLOW CALCULATIONS FOR VARIOUS
INITIAL POINTS USING THE QUADRATIC FORM.

Forms	Case study	Initial $Value \times$	Iterations	Residual	Number of operations
	18 - BusPower	1	4	5.03e - 22	260
	Distribution	±20	12	2.90e - 16	676
	System	±100	16	3.94e - 16	884
	22 - bus Power	1	5	3.46e - 14	384
	Distribution	±20	12	4.21e - 19	832
	System	±100	16	5.98e - 20	1088
ati d	69 - bus Power	1	9	9.33e - 08	2050
Convex Quadrati form	Distribution	±20	17	7.64e - 08	3690
Convex Quadratic form	System	±100	21	1.18e - 07	4510
	85 - bus Power	1	5	5.38e - 16	1518
	Distribution	±20	13	1.64e - 13	3542
	System	±100	17	6.62e - 12	4554
	141 - bus Power	1	16	4.16e - 11	6737
	Distribution	±20	33	4.28e - 08	12634
	System	±100	27	5.92e - 11	11368
	IEEE $906 - Bus$	1	11	2.141e - 07	32592
	European	±20	18	3.11e - 07	51604
	Test Feeder	±100	24	7.61e - 07	65185

quadratic form has significantly improved as compared to the calculations based on the polar form.

3) The Effect of Deviant Initial Conditions: Table IV provides the results of the power flow calculations based on the quadratic form for highly deviant initial points. The simulation results show that the quadratic form is robust to deviant initial points. When the initial values are increased 20 and 100 times, the number of iterations and of operations typically increases a little.

VI. CONCLUSIONS

In this paper, we present a new transformation of the AC power flow equations. Our proposed algorithm significantly alleviate the fractal behavior. We show that our approach is robust to heavy loads, high values of the line resistances and reactances, and deviant initial points. The performance the AC power flow calculations are significantly improved. As for the residuals, they are decreased by $3.785 \times 10^{+20}$ when using the proposed convex quadratic form. The number of the iterations and of the operations are decreased 716 and 384 times in some scenarios.

REFERENCES

- E. E. Pompodakis, G. C. Kryonidis, and M. C. Alexiadis, "A comprehensive load flow approach for grid-connected and islanded ac microgrids," *IEEE Transactions on Power Systems*, vol. 35, no. 2, pp. 1143–1155, 2020.
- [2] S. D. Varwandkar, "Realification of power flow," *IEEE Transactions on Power Systems*, vol. 34, no. 3, pp. 2433–2440, 2019.
- [3] Y. Xu, L. Mili, and J. Zhao, "Probabilistic power flow calculation and variance analysis based on hierarchical adaptive polynomial chaos-anova method," *IEEE Transactions on Power Systems*, vol. 34, no. 5, pp. 3316– 3325, 2019.
- [4] M. Tostado-Véliz, S. Kamel, and F. Jurado, "A robust power flow algorithm based on bulirsch–stoer method," *IEEE Transactions on Power Systems*, vol. 34, no. 4, pp. 3081–3089, 2019.
- [5] K. Tang, S. Dong, J. Shen, C. Zhu, and Y. Song, "A robust and efficient two-stage algorithm for power flow calculation of large-scale systems," *IEEE Transactions on Power Systems*, vol. 34, no. 6, pp. 5012–5022, 2019
- [6] Z. Yang, K. Xie, J. Yu, H. Zhong, N. Zhang, and Q. Xia, "A general for-mulation of linear power flow models: Basic theory and error analysis," *IEEE Transactions on Power Systems*, vol. 34, no. 2, pp. 1315–1324, 2018
- [7] D. Shchetinin, T. T. De Rubira, and G. Hug, "On the construction of linear approximations of line flow constraints for ac optimal power flow," *IEEE Transactions on Power Systems*, vol. 34, no. 2, pp. 1182–1192, 2018
- [8] A. Venzke and S. Chatzivasileiadis, "Convex relaxations of probabilistic ac optimal power flow for interconnected ac and hvdc grids," *IEEE Transactions on Power Systems*, vol. 34, no. 4, pp. 2706–2718, 2019.
- [9] Y. Xu, Z. Hu, L. Mili, M. Korkali, and X. Chen, "Probabilistic power-flow calculation based on a novel gaussian process emulator," *IEEE Transactions on Power Systems*, pp. 1–1, 2020.
- [10] B. I. Epureanu and H. S. Greenside, "Fractal basins of attraction associated with a damped newton's method," SIAM review, pp. 102– 109 1998
- [11] J. S. Thorp and S. A. Naqavi, "Load-flow fractals draw clues to erratic behaviour," *IEEE Computer Applications in Power*, vol. 10, no. 1, pp. 59–62, 1997.
- [12] B. B. Mandelbrot, The fractal geometry of nature. WH freeman New York, 1983, vol. 173.
- [13] D. L. Turcotte, Fractals and chaos in geology and geophysics. Cambridge university press, 1997.
- [14] R. H. Byrd, J. C. Gilbert, and J. Nocedal, "A trust region method based on interior point techniques for nonlinear programming," *Mathematical programming*, vol. 89, no. 1, pp. 149–185, 2000.
- [15] J. J. Moré and D. C. Sorensen, "Computing a trust region step," SIAM Journal on Scientific and Statistical Computing, vol. 4, no. 3, pp. 553– 572, 1983.
- [16] C. W. C4.605, "Modelling and aggregation of loads in flexible power networks," Cigre, Tech. Rep., 2014.
- [17] W. M. Grady, M. Samotyj, and A. Noyola, "The application of network objective functions for actively minimizing the impact of voltage harmonics in power systems," *IEEE transactions on power delivery*, vol. 7, no. 3, pp. 1379–1386, 1992.
- [18] M. R. Raju, K. R. Murthy, and K. Ravindra, "Direct search algorithm for capacitive compensation in radial distribution systems," *International Journal of Electrical Power & Energy Systems*, vol. 42, no. 1, pp. 24–30, 2012.
- [19] D. Das, "Optimal placement of capacitors in radial distribution system using a fuzzy-ga method," *International Journal of Electrical Power & Energy Systems*, vol. 30, no. 6-7, pp. 361–367, 2008.
- [20] D. Das, D. Kothari, and A. Kalam, "Simple and efficient method for load flow solution of radial distribution networks," *International Journal of Electrical Power & Energy Systems*, vol. 17, no. 5, pp. 335–346, 1995.
- [21] H. Khodr, F. Olsina, P. De Oliveira-De Jesus, and J. Yusta, "Maximum savings approach for location and sizing of capacitors in distribution systems," *Electric Power Systems Research*, vol. 78, no. 7, pp. 1192– 1203, 2008.
- [22] D. T. Feeders, "Ieee pes distribution system analysis subcommittee," OnlineAvailable: http://www. ewh. ieee. org/soc/pes/dsacom/testfeeders/index. html, 2011.